



## Continuum limits of bistable spring models of carbon nanotube arrays accounting for material damage

T. Blesgen<sup>a,\*</sup>, F. Fraternali<sup>b</sup>, J.R. Raney<sup>c</sup>, A. Amendola<sup>b</sup>, C. Daraio<sup>c</sup>

<sup>a</sup> Max-Planck-Institute for Mathematics in the Sciences, Inselstraße 22-26, D-04103 Leipzig, Germany

<sup>b</sup> Department of Civil Engineering, University of Salerno, 84084 Fisciano (SA), Italy

<sup>c</sup> Engineering and Applied Science, California Institute of Technology, Pasadena, CA 91125, USA

### ARTICLE INFO

#### Article history:

Received 5 December 2011

Received in revised form 15 July 2012

Available online 27 July 2012

#### Keywords:

Carbon nanotube arrays

Bistable springs

Multiscale behavior

Mullins effect

Permanent deformation

### ABSTRACT

Using chains of bistable springs, a model is derived to investigate the plastic behavior of carbon nanotube arrays with damage. We study the preconditioning effect due to the loading history by computing analytically the stress–strain pattern corresponding to a fatigue-type damage of the structure. We identify the convergence of the discrete response to the limiting case of infinitely many springs, both analytically in the framework of Gamma-convergence, as well as numerically.

© 2012 Elsevier Ltd. All rights reserved.

### 1. Introduction

Because of their interesting combination of properties, including high strength, low density, and high electrical and thermal conductivities, carbon nanotubes (CNTs) have been of great interest as nanoscale elements in a variety of applications (Baughman et al., 2002). Aligned arrays of CNTs can be readily synthesized to form foam-like materials that combine low density with a desirable dissipative response (Cao et al., 2005; Gibson and Ashby, 1999).

There are a few interesting structural and mechanical features of these materials: first, the thermal chemical vapor deposition process that is typically used to synthesize the arrays (Cao et al., 2005) results in a gradient in physical properties (such as density) along the height of the structure. This leads to strain localization during compression, with the majority of the structure remaining undeformed while increasing strain results in the sequential addition of highly localized buckles (Yaglioglu, 2007; Hutchens et al., 2010). Second, there is a large amount of strain recovery after compression (typical of the CNT arrays that we study, which are synthesized using a vapor phase catalyst (Cao et al., 2005), but not for all types of CNT arrays that are synthesized differently (Yaglioglu, 2007; Bradford et al., 2011)). Third, the stress–strain

response of the material is hysteretic, with different loading and unloading paths. It has been noted in the past that repeated compressive cycles result in a hysteresis of decreasing area and decreasing stress at any given strain for the first few cycles (Cao et al., 2005). This effect, sometimes referred to as *preconditioning*, ceases after the initial few cycles, resulting in a hysteresis of constant area for loading cycles thereafter. Finally, we observe that this preconditioning effect is dependent on the maximum strain reached. When the maximum strain of all previous loading cycles is exceeded, the stress response obtained at these elevated strains is that of the un-preconditioned material, as if it had never been compressed previously (Misra et al., 2009).

The features we have enumerated for the foam-like response of CNT arrays are analogous to those observed in other soft materials such as filled rubbers. In the context of rubbers, this response is associated with what is termed the *Mullins effect* (Mullins, 1947; Dorfmann and Ogden, 2004). Capturing these features simultaneously in models has proven difficult in the past for other materials, with frequent use of simplifying assumptions that only allow models to match some of the experimental observations (see, e.g., the *idealized Mullins effect* modeled by De Tommasi and Puglisi, 2006).

We show in the present work that a suitable generalization of the mesoscopic mass-spring model of CNT structures recently proposed by Fraternali et al. (2010) is able to handle the material damage due to preconditioning and permanent deformation within an effective one-dimensional framework. We introduce preconditioning-induced material damage by setting to zero the

\* Corresponding author.

E-mail addresses: [blesgen@mis.mpg.de](mailto:blesgen@mis.mpg.de) (T. Blesgen), [f.fraternali@unisa.it](mailto:f.fraternali@unisa.it) (F. Fraternali), [raney@caltech.edu](mailto:raney@caltech.edu) (J.R. Raney), [adamendola@gmail.com](mailto:adamendola@gmail.com) (A. Amendola), [daraio@caltech.edu](mailto:daraio@caltech.edu) (C. Daraio).

stiffness of a suitable percentage of the bistable springs that describe the response of the material at the microscopic scale. This allows us to model permanent axial deformation of the structure through the irreversible ‘annihilation’ of the springs with zero stiffness.

## 2. Multiscale mass-spring models of CNT arrays

### 2.1. Bistable spring model at the microscopic scale

We model an infinitesimal portion of a CNT foam through the bistable spring model described in Fraternali et al. (2010), which we hereafter briefly summarize. We assume that such a portion of the foam can be described as a chain of  $N + 1$  lumped masses  $m^0, \dots, m^N$ , with  $m^0$  clamped at the bottom of the chain. The adjacent masses are connected to each other through bistable springs characterized by the axial strains

$$\varepsilon^i = \varepsilon^i(u_N) = \frac{u_N^{i-1} - u_N^i}{h_N}, \quad i = 1, \dots, N \quad (1)$$

where  $u_N^i$  is the axial displacement of the mass  $m^i$  (positive upward),  $h_N := L/N$  is the equal spacing between the masses, and  $u_N := \{u_N^0, \dots, u_N^N\}$ . The potential  $V^i$  and stress  $\sigma^i$  vs strain  $\varepsilon^i$  laws of the generic spring are

$$V^i(\varepsilon^i) := \begin{cases} V_a^i(\varepsilon^i) := -k_0^i[\varepsilon^i + \ln(1 - \varepsilon^i)], & \varepsilon^i < \varepsilon_a^i, \\ V_b^i(\varepsilon^i) := c_1 + \sigma_a^i \varepsilon^i + \frac{1}{2} k_b^i (\varepsilon^i - \varepsilon_a^i)^2, & \varepsilon_a^i \leq \varepsilon^i \leq \bar{\varepsilon}_c^i, \\ V_c^i(\varepsilon^i) := c_2 - k_c^i[\varepsilon^i - \varepsilon_c^i + \ln(1 - (\varepsilon^i - \varepsilon_c^i))], & \bar{\varepsilon}_c^i < \varepsilon^i, \end{cases} \quad (2)$$

$$\sigma^i(\varepsilon^i) = V^i(\varepsilon^i) = \begin{cases} k_0^i \frac{\varepsilon^i}{1 - \varepsilon^i}, & \varepsilon^i < \varepsilon_a^i, \\ \sigma_a^i + k_b^i (\varepsilon^i - \varepsilon_a^i), & \varepsilon_a^i \leq \varepsilon^i \leq \bar{\varepsilon}_c^i, \\ \frac{k_c^i (\varepsilon^i - \varepsilon_c^i)}{1 - (\varepsilon^i - \varepsilon_c^i)}, & \bar{\varepsilon}_c^i < \varepsilon^i \end{cases} \quad (3)$$

where  $k_0^i > 0$ ,  $k_b^i < 0$ ,  $k_c^i > 0$ ,  $\varepsilon_a^i > 0$  and  $\varepsilon_c^i \geq \varepsilon_a^i$  are constitutive parameters (five independent parameters); the constants  $c_1 < 0$  and  $c_2 > 0$  are such that  $V_a^i(\varepsilon_a^i) = V_b^i(\varepsilon_a^i)$ ,  $V_b^i(\bar{\varepsilon}_c^i) = V_c^i(\bar{\varepsilon}_c^i)$ ; and it results (compare with Figs. 2 and 3 of Fraternali et al., 2010 for the notation)

$$\varepsilon_c^i = \varepsilon_c^i - \frac{\sigma_a^i}{k_c^i + \sigma_a^i}, \quad \bar{\varepsilon}_c^i = \frac{\varepsilon_c^i (k_c^i + \sigma_a^i)}{k_c^i + \sigma_c^i} + \frac{(\sigma_c^i - \sigma_a^i)(k_c^i + \varepsilon_c^i k_c^i + \varepsilon_c^i \sigma_a^i)}{(k_c^i + \sigma_a^i)(k_c^i + \sigma_c^i)} \quad (4)$$

$$\text{with } \sigma_a^i = k_0^i(\varepsilon_a^i/(1 - \varepsilon_a^i)), \quad \sigma_c^i = \sigma_a^i + k_b^i(\bar{\varepsilon}_c^i - \varepsilon_a^i).$$

### 2.2. Plasticity and damage

At the microscopic scale, the bistable springs introduced above permit a dynamic switching process between the phases (a) and (c), cf. Puglisi and Truskinovsky (2002, 2005). As in Puglisi and Truskinovsky (2005), we name a response of the material *plastic*, if the strain  $\varepsilon^i$  of a single spring exceeds the threshold  $\varepsilon_a^i$ . For a chain of  $N$  springs, this can be characterized by the occurrence of loading and unloading stress plateaux.

Within the current section, we rescale for simplicity  $L$  to unity; name (b) the unstable phase; and regard a mesoscopic element of a CNT array as the limit  $N \rightarrow \infty$  of a series of  $N$  microscopic springs.

Let  $m$  denote the number of hysteresis cycles that have been applied to the material during the previous loading history (up to different maximum strains). We assume that such a loading path has severely weakened the stiffness of  $(1 - \beta(m))N$  microscopic

springs, for given  $0 < \beta(m) \leq 1$ , and that at the current time it holds for all  $m \in \mathbb{N}$

$$(A1) \quad k_c^i = k_0^i \quad \text{for all } i \in \mathbb{N}$$

$$(A2) \quad k_0^1 = k_0^2 = \dots = k_0^{\lfloor \beta N \rfloor} = k_0, \quad k_0^{\lfloor \beta N \rfloor + 1} = \dots = k_0^N = \delta$$

$$(A3) \quad \varepsilon_*^i = \varepsilon_* \quad \text{for } i = 1, \dots, \beta N$$

$$(A4) \quad \varepsilon_a^i = \bar{\varepsilon}_c^i \quad \text{for } i = \beta N + 1, \dots, N.$$

Condition (A1) stipulates the *symmetry* of the microscopic springs. (A2) states that the springs  $\lfloor \beta N \rfloor + 1$  to  $N$  have stiffness  $k_0^i = \delta$ , where  $\delta > 0$  is a small constant (*damaged springs*). We name *undamaged* those springs with stiffness constant  $k_0$  (springs 1 to  $\beta N$ ).

With  $V^i$  given by (2), the mechanical energy of the structure is

$$E_N(u_N) := \frac{1}{N} \sum_{i=1}^N V^i(\varepsilon^i(u_N)).$$

Let  $\sigma$  be the given total stress. The mesoscopic average strain is simply  $\varepsilon(u_N) := (1/N) \sum_{i=1}^N \varepsilon^i(u_N)$ , where  $\varepsilon^i$  denotes the strain associated with the  $i$ th spring. Following an original idea of Puglisi and Truskinovsky (2005), we model plasticity by the gradient flow equations

$$v \dot{\varepsilon}^i(u_N) = - \frac{\partial \Phi_N}{\partial \varepsilon^i}(\varepsilon^1(u_N), \dots, \varepsilon^N(u_N)) \quad (5)$$

with the total energy

$$\Phi_N(\varepsilon^1, \dots, \varepsilon^N) := \frac{1}{N} \sum_{i=1}^N [V^i(\varepsilon^i) - \sigma \varepsilon^i].$$

The evolution equation (5) lets  $\varepsilon^i$  evolve towards local minimizers of  $\Phi_N$ . We are interested in the limit  $v \rightarrow 0$  which amounts to infinitely fast evolution such that  $\varepsilon(u_N)$  attains a local minimizer of  $\Phi_N$ . First we construct the equilibrium points. Inside the  $i$ th spring element, the strain must satisfy the condition  $(V^i)'(\varepsilon^i) = \sigma$ . For given total stress  $\sigma$ , there are at most the three local minimizers (using (A3))

$$\tilde{\varepsilon}_a^i(m) = \frac{\sigma}{k_0^i + \sigma}, \quad \tilde{\varepsilon}_b^i(m) = \frac{\sigma - \sigma_a}{k_b^i} + \varepsilon_a^i, \quad (6a)$$

$$\tilde{\varepsilon}_c^i(m) = \frac{\sigma(1 + \varepsilon_*) + k_0^i \varepsilon_*}{k_0^i + \sigma} = \tilde{\varepsilon}_a^i(m) + \varepsilon_*. \quad (6b)$$

Note that for the derivation of (6), we require that  $\delta$  is positive.

In a loading or unloading experiment, the first spring located closer to the bottom of the structure is the softest and yields first, changing its phase, Raney et al. (2011a). Next, the second spring yields, and so forth, until the  $\beta N$ th spring. (Note that in accordance with (A4), the springs  $\beta N + 1, \dots, N$  with small spring constant  $\delta$  do not flip.) Therefore, similar to the case of  $N$  identical springs, the total state of the series of springs is still completely specified by two scalar parameters  $p$  and  $q$  and the additional parameter  $\beta$ . Here,  $p, q, 1 - p - q$  denote the phase fractions of the minimizers  $a, b$ , and  $c$ , which corresponds to having  $\beta N p, \beta N q$  and  $\beta N(1 - p - q)$  springs in phase  $a, b$ , and  $c$ , respectively. We assumed here that  $\beta N p \in \mathbb{N}$ .

As  $\varepsilon \mapsto V^i(\varepsilon)$  is concave in Regime  $b$  for all  $i \in \mathbb{N}$ , if the elongation of a spring in the local minimum  $\tilde{\varepsilon}_b^i$  is altered by an arbitrarily small perturbation, it will move (according to the sign of the perturbation) to either  $\tilde{\varepsilon}_a^i$  or  $\tilde{\varepsilon}_c^i$ . As a consequence, any system of  $N$  springs with  $q \neq 0$  is unstable and we may in the following restrict to the case  $q = 0$ .

The average strain of a system with  $\beta N$  springs in equilibrium and the first  $\beta N p$  springs in phase a fulfills the identity

$$\varepsilon(m) = \frac{1}{N} \sum_{i=1}^{\beta N} \tilde{\varepsilon}_a^i(m) + \frac{1}{N} \sum_{i=\beta N p+1}^{\beta N} \varepsilon_* + \frac{1}{N} \sum_{i=\beta N+1}^N \frac{\sigma}{\delta + \sigma}.$$

Here we only study the limiting case  $\delta \searrow 0$  where there is no further small correction of the damaged springs. In this case, we obtain

$$\begin{aligned} \varepsilon(m) &= \frac{\beta \sigma(m)}{k_0 + \sigma(m)} + (1 - \beta) + \beta(1 - p)\varepsilon_* \\ &= \frac{\sigma(m) + (1 - \beta)k_0}{k_0 + \sigma(m)} + \beta(1 - p)\varepsilon_*, \end{aligned} \tag{7}$$

where we used (A1)–(A4), (3) and (6); especially  $\tilde{\varepsilon}_c^i = \tilde{\varepsilon}_a^i + \varepsilon_*$ .

Resolving (7), we get the stress–strain relationship for a  $N$ -springs system

$$\sigma(\varepsilon, m) = \frac{k_0(\varepsilon - \varepsilon_p + \beta - 1)}{1 - (\varepsilon - \varepsilon_p)} \tag{8}$$

with  $\varepsilon_p(m) := \beta(1 - p)\varepsilon_*$ . The latter can in a natural way be identified with the plastic strain. From (8) we see that  $\sigma$  only depends on  $m$  and on the elastic strain  $\varepsilon_{el} := \varepsilon - \varepsilon_p$ .

### 2.3. Analytic computation of the continuum limit

We identify the continuum limit of  $E_N$  in the framework of  $\Gamma$ -convergence (see, e.g., Braides, 2002). This is not a standard procedure as  $V$  also depends on the spatial position.

Let  $L=1$  (which can always be obtained by rescaling), and  $\Omega := (0, 1)$ . For prescribed  $l > 0$ , we impose the boundary conditions

$$u_0^N = 0, \quad u_1^N = l. \tag{9}$$

We now specify our assumptions on  $V$ . The mechanical pair-potential is a function of the deformation gradient. In addition, in order to capture the effect of damage expressed in the assumptions (A1)–(A4) above, we need to respect the dependence of  $V$  on the spatial position  $i$ . Let  $\text{dom}(V) = [0, 1] \times D$  for suitable  $D \subset \mathbb{R}$  be the domain of definition of  $V$ . We postulate the following conditions on  $V$ .

(COND 1) There exist positive constants  $c_1, C_1$ , such that

$$c_1(|\varepsilon| - 1) \leq V(x, \varepsilon) \leq C_1(|\varepsilon| + 1) \quad \text{for all } (x, \varepsilon) \in [0, 1] \times D.$$

(COND 2) The function  $x \mapsto V(x, \varepsilon)$  is continuous for any  $\varepsilon \in D$ .

After extending  $V$  given by (2) continuously in  $i$  by interpolation, we easily verify that this extension (again called  $V$ ) satisfies both COND 1 and COND 2. For given deformations  $u_N := (u_i^N)_{0 \leq i \leq N}$ , we may rewrite the overall mechanical energy of the chain as a functional of the discrete displacement gradient,

$$E_N(u_N) := h_N \sum_{i=0}^{N-1} V\left(\frac{i}{N}, \frac{u_{i+1}^N - u_i^N}{h_N}\right). \tag{10}$$

The functional  $V$  coincides with (2), but the dependence on the subscript  $i$  has moved to the first argument. We scaled  $E_N$  by  $h_N$  as we are dealing with a microscopic energy.

Following ideas in Braides et al. (1999), we introduce for  $N \in \mathbb{N}$  the set  $\mathcal{A}_N$  of all functions  $u : h_N \mathbb{Z} \cap [0, 1] \rightarrow \mathbb{R}$ , setting  $u_i := u(ih_N)$ . We tacitly identify  $\mathcal{A}(0, 1)$  with the piecewise affine linear interpolations, i.e.

$$\begin{aligned} \mathcal{A}(0, 1) &:= \{u : [0, 1] \rightarrow \mathbb{R} \mid u \text{ is affine in } (ih_N, (i+1)h_N), \\ &0 \leq i \leq N-1\}. \end{aligned}$$

With  $u_i = u(ih_N)$ , as a shorthand notation for the second argument in (10), we introduce the symbol

$$\nabla^N u_N(x) := \frac{u_{i+1}^N - u_i^N}{h_N}, \quad x \in [ih_N, (i+1)h_N), \quad 0 \leq i \leq N-1,$$

which is a discrete approximation of  $\nabla u$  with step size  $h_N$ .

For later use we introduce  $E_N^l : \mathcal{A}(0, 1) \rightarrow \mathbb{R} \cup \{+\infty\}$  by

$$E_N^l(u) := \begin{cases} E_N(u), & \text{if } u(0) = 0, u(1) = l, \\ +\infty, & \text{otherwise.} \end{cases}$$

**Theorem 1** (Continuum limit of  $E_N$ ). *Let  $V$  satisfy the conditions (COND 1), (COND 2) and let  $l > 0$ . Then the functional  $E_N^l$  converges in the  $\Gamma$ -sense for  $N \rightarrow \infty$  to a functional  $E^l : L^1(0, 1) \rightarrow \mathbb{R}$  defined by*

$$E^l(u) := \begin{cases} \int_0^1 V_0^{**}(x, \nabla u(x)) \, dx & \text{if } u \in H^{1,1}(0, 1), u(0) = 0, u(1) = l, \\ +\infty & \text{else.} \end{cases}$$

Here,  $V_0(x, z) := \frac{1}{2} \min \{V(x, z_1) + V(x, z_2) \mid z_1 + z_2 = 2z\}$ , and  $V_0^{**}$  denotes the convexification of  $V_0$  (see, e.g., Rockafellar, 1997).

**Proof.**

(a) *Proof of the lim inf-inequality.*

Let a sequence  $(u_N)_{N \in \mathbb{N}} \subset L^1(0, 1)$  be given with  $u_N \rightarrow u$  in  $L^1(0, 1)$  as  $N \rightarrow \infty$ . W.l.o.g.  $E_N^l(u_N) < \infty$  and thus  $E_N(u_N) < \infty$ . Now, as the bounds in (COND 1) are uniform in  $x$ , we can apply Theorem 2 in Blesgen (2007) which proves the lim inf-inequality for  $(u_N)_N$ .

(b) *Proof of the lim sup-inequality.*

Let  $u \in L^1(0, 1)$  be given. We have to show the existence of a sequence  $(u_N)_{N \in \mathbb{N}} \subset L^1(0, 1)$  such that  $u_N \rightarrow u$  in  $L^1(0, 1)$  as  $N \rightarrow \infty$  and

$$\limsup_{N \rightarrow \infty} E_N^l(u_N) \leq E^l(u).$$

By a standard density argument, cf. Part (b3) in the proof of Theorem 2 in Blesgen (2007), we may restrict to the affine case  $u(x) = ax + b$ .

For the construction we first ignore the boundary conditions (9). Let  $N = km$  for some  $m, k \in \mathbb{N}$ . We will choose functions  $u_N$  which are periodic in any subinterval of  $(0, 1)$  with length  $mh_N$ . We write the integrand as  $V(d_N(x), \cdot)$ , where  $d_N : (0, 1) \rightarrow \mathbb{R}$  is a piecewise constant bounded function with  $d_N \rightarrow \text{Id}$  for  $N \rightarrow \infty$ . The method can be generalized to more general situations. With these settings we find

$$E_N(u_N) = \sum_{i=0}^{k-1} \int_{imh_N}^{(i+1)mh_N} V(d^i, \nabla^N u_N(x)) \, dx + o(1), \tag{11}$$

where  $d^i := d_N((i+1/2)mh_N)$ ; and (COND 2) has been used.

By convexity of  $V_0^{**}$  and Carathéodory's theorem (see, e.g., Rockafellar, 1997) we know that for any  $0 \leq i \leq k-1$ , there exist real numbers  $\lambda_1, \lambda_2$  with  $0 \leq \lambda_1, \lambda_2 \leq 1$  and  $0 \leq \lambda_1 + \lambda_2 \leq 1$  such that

$$\begin{aligned} V_0^{**}(d^i, a) &= \lambda_1 V_0(d^{1,i}, a^1) + \lambda_2 V_0(d^{2,i}, a^2) \\ &+ (1 - \lambda_1 - \lambda_2) V_0(d^{3,i}, a^3), \end{aligned} \tag{12}$$

$$\begin{aligned} (d^i, a) = (d^i, \nabla u) &= \lambda_1 (d^{1,i}, a^1) + \lambda_2 (d^{2,i}, a^2) \\ &+ (1 - \lambda_1 - \lambda_2) (d^{3,i}, a^3). \end{aligned} \tag{13}$$

For given  $\lambda_1, \lambda_2$  we introduce the sets

$$\begin{aligned} \Omega_1^N &:= \Omega \cap \cup_{i=0}^{k-1} (ihm, ihm + h\lfloor \lambda_1 m \rfloor], \\ \Omega_2^N &:= \Omega \cap \cup_{i=0}^{k-1} ((ihm + h\lfloor \lambda_1 m \rfloor), (ihm + h\lfloor (\lambda_1 + \lambda_2) m \rfloor]), \\ \Omega_3^N &:= \Omega \cap \cup_{i=0}^{k-1} ((ihm + h\lfloor (\lambda_1 + \lambda_2) m \rfloor), (i + 1)hm], \end{aligned}$$

such that  $\Omega = \Omega_1^N \cup \Omega_2^N \cup \Omega_3^N$ .

By definition of  $V_0$  it holds for  $0 \leq i \leq k - 1$  and any  $s = 1, 2, 3$ ,

$$V_0(d^{s,i}, a^s) = \frac{1}{2} [V(d_1^{s,i}, a_1^s) + V(d_2^{s,i}, a_2^s)],$$

where  $d^{s,i}, a^s, 1 \leq s \leq 3$ , are suitable numbers such that  $d^{s,i} = (d_1^{s,i} + d_2^{s,i})/2$  and  $a^s = (a_1^s + a_2^s)/2$ . We choose  $u_N(x) = a_N(x)x + b$ , where

$$a_N(x) = \begin{cases} a_1^1, & \text{if } x \in \Omega_1^N \cap \cup_{i=0}^{k-1} \cup_{j=0}^{m/2-1} ((im + 2j)h_N, (im + 2j + 1)h_N], \\ a_2^1, & \text{if } x \in \Omega_2^N \cap \cup_{i=0}^{k-1} \cup_{j=0}^{m/2-1} ((im + 2j)h_N, (im + 2j + 1)h_N], \\ a_3^1, & \text{if } x \in \Omega_3^N \cap \cup_{i=0}^{k-1} \cup_{j=0}^{m/2-1} ((im + 2j)h_N, (im + 2j + 1)h_N], \\ a_1^2, & \text{if } x \in \Omega_1^N \cap \cup_{i=0}^{k-1} \cup_{j=0}^{m/2-1} ((im + 2j + 1)h_N, (im + 2j + 2)h_N], \\ a_2^2, & \text{if } x \in \Omega_2^N \cap \cup_{i=0}^{k-1} \cup_{j=0}^{m/2-1} ((im + 2j + 1)h_N, (im + 2j + 2)h_N], \\ a_3^2, & \text{if } x \in \Omega_3^N \cap \cup_{i=0}^{k-1} \cup_{j=0}^{m/2-1} ((im + 2j + 1)h_N, (im + 2j + 2)h_N]. \end{cases}$$

For  $s = 1, 2, 3$  and  $0 \leq i \leq k - 1$  we set

$$d_N(x) = \begin{cases} d_1^{s,i}, & \text{if } x \in \Omega_s^N \cap \cup_{i=0}^{k-1} \cup_{j=0}^{m/2-1} ((im + 2j)h_N, (im + 2j + 1)h_N], \\ d_2^{s,i}, & \text{if } x \in \Omega_s^N \cap \cup_{i=0}^{k-1} \cup_{j=0}^{m/2-1} ((im + 2j + 1)h_N, (im + 2j + 2)h_N]. \end{cases}$$

The ansatz for  $d_N$  depends on the current interval, as  $V$  is  $x$ -dependent.

Eqn. (11) now reads after setting  $\lfloor \lambda_s m \rfloor := m - \lfloor \lambda_1 m \rfloor - \lfloor \lambda_2 m \rfloor$  for short

$$\begin{aligned} E_N(u_N) &= h_N \sum_{i=0}^{k-1} \sum_{s=1}^3 \lfloor \lambda_s m \rfloor \frac{1}{2} [V(d_1^{s,i}, a_1^s) + V(d_2^{s,i}, a_2^s)] \\ &= \sum_{i=0}^{k-1} - \sum_{s=1}^3 \frac{\lfloor \lambda_s m \rfloor}{m} V_0(d^{s,i}, a^s). \end{aligned} \tag{14}$$

For  $m \rightarrow \infty$  we have  $\lfloor \lambda_s m \rfloor / m \rightarrow \lambda_s, s = 1, 2$ . Consequently, using (12),

$$E_N(u_N) \rightarrow \int_0^1 V_0^{***}(x, \nabla u(x)) dx = E^l(u) \quad \text{as } N \rightarrow \infty.$$

We still have to show that  $u_N \rightarrow u$  in  $L^1(0, 1)$ . If in the derivation of Eqn. (14) we formally set  $V(x, v) := v$  (which is feasible), we obtain

$$\int_0^1 \nabla u_N(x) dx = \frac{\lfloor \lambda_1 m \rfloor}{m} a^1 + \frac{\lfloor \lambda_2 m \rfloor}{m} a^2 + (1 - \frac{\lfloor \lambda_1 m \rfloor}{m} - \frac{\lfloor \lambda_2 m \rfloor}{m}) a^3$$

and in the limit  $m \rightarrow \infty$  as above

$$\begin{aligned} \lim_{N \rightarrow \infty} \int_0^1 \nabla u_N(x) dx &= \lambda_1 a^1 + \lambda_2 a^2 + (1 - \lambda_1 - \lambda_2) a^3 \\ &= a = \int_0^1 \nabla u(x) dx, \end{aligned} \tag{15}$$

where Eqn. (13) has been used. By (15),  $u_N \rightarrow u$  in  $L^r(0, 1)$  for  $1 \leq r \leq \infty$ .

We still need to incorporate the boundary condition (9). If  $u_N$  is the recovery sequence from above, we define

$$v_N(x) := \begin{cases} \frac{u_N(h_N)}{h_N} x, & x \in [0, h_N], \\ u_N(x), & x \in [h_N, 1 - h_N], \\ \frac{l - u_N(1 - h_N)}{h_N} (x - 1) + l, & x \in (1 - h_N, 1]. \end{cases}$$

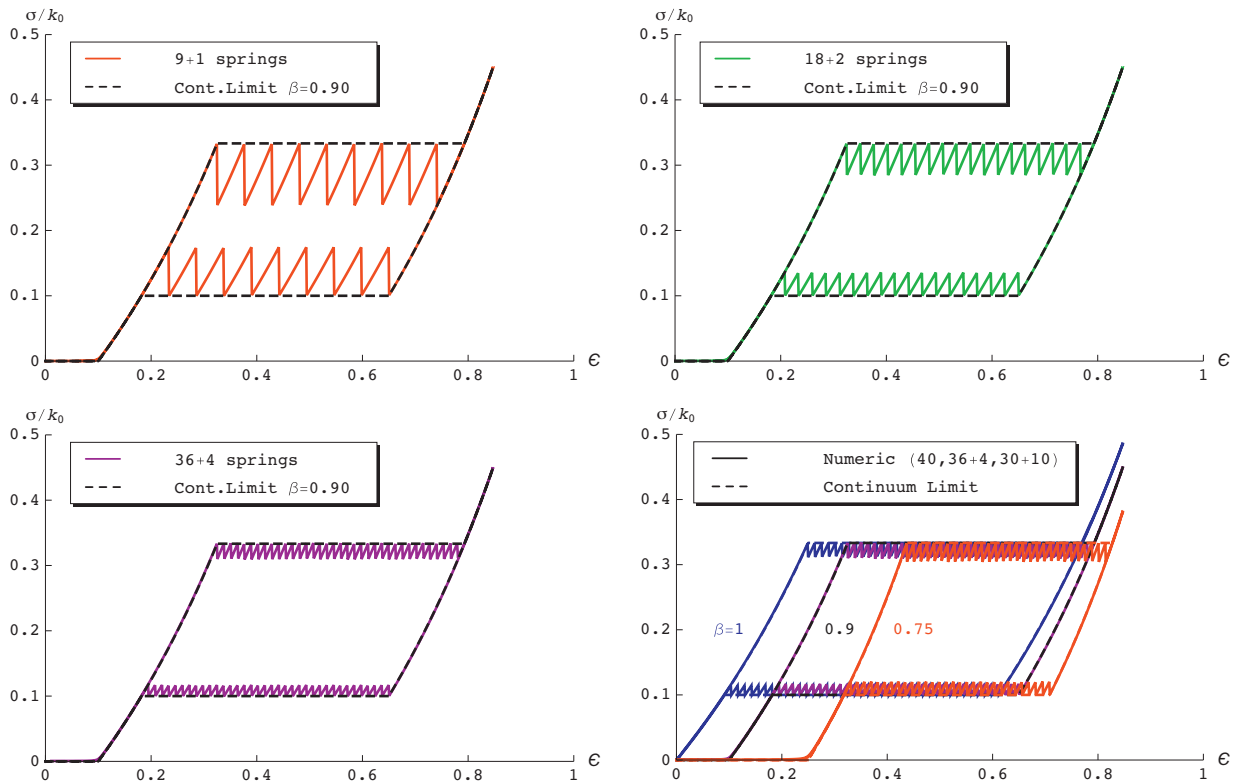
By construction,  $v_N$  is continuous on  $[0, 1]$  with  $v_N(0) = 0, v_N(1) = l$ , and  $\lim_{N \rightarrow \infty} (E_N(u_N) - E_N(v_N)) = 0$ , which shows that  $v_N$  is the sought recovery sequence.  $\square$

### 3. Numerical results

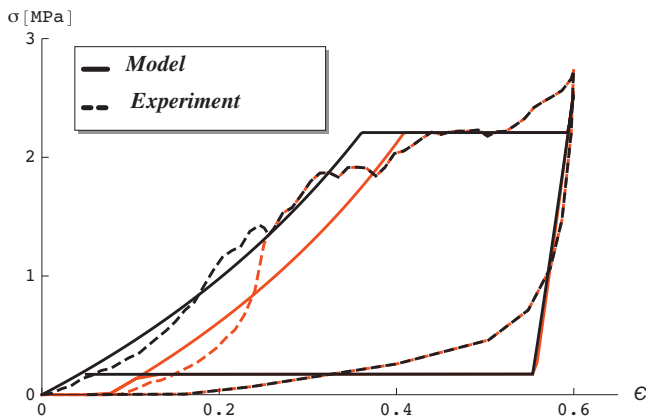
We study in this section the numerical convergence of the stress–strain response of finite mass-spring systems to the continuum limit of Eqn. (8). We analyze the overall loading–unloading response of discrete systems composed of  $N = x + y$  springs, where  $x$  denotes the number of undamaged springs, while  $y$  specifies the number of damaged springs. For the spring constants, we use the parameters  $k_0 = 50.00 \times 10^6$  Pa,  $k_b = -22.44 \times 10^6$  Pa,  $\varepsilon_a = 0.25$ ,  $\varepsilon_* = 0.52$ ,  $\delta = 50.00 \times 10^2$  Pa, which correspond to  $\sigma_a = 16.67$  MPa,  $\sigma_c = 5.00$  MPa, and  $\Delta\sigma = \sigma_c - \sigma_a = -11.67$  MPa.

Fig. 1 shows the results for different  $x, y$ . The stress–strain curves of the discrete microscopic chains follow sawtooth patterns which alternate *elastic* and *plastic* steps. The plastic steps are characterized by fixed total strain and microscopic branch switching. Such sawtooth-like responses converge to a perfectly plastic behavior with a loading ( $\sigma = \sigma_a$ ) and an unloading plateau ( $\sigma = \sigma_c$ ) for increasing values of  $N$ , as predicted by Eqn. (8). It is worth observing that the stress is zero for  $\varepsilon \leq 1 - \beta$ , while for  $\varepsilon > 1 - \beta$  that the system is able to bear stresses  $\sigma > 0$ . Fig. 1 shows, in addition, that the energy dissipation capacity of the system (proportional to the area enclosed by the stress–strain curve in a loading–unloading cycle) reduces for decreasing  $\beta$ , that is for increasing number of damaged springs (bottom-right panel). Remarkably, the quantity  $1 - \beta$  can be regarded as the ‘activation’ strain of the system.

The dashed curves shown in Fig. 2 provide some data to allow for a comparison between the continuum limit of the model given in Section 2.1 (for  $k_c \neq k_0$ ) and an actual experiment. A CNT array sample was synthesized following the procedures discussed in detail in Raney et al. (2011b). The mechanical response given in Fig. 2 was obtained by compressing the material first to a moderate strain of  $\varepsilon = 0.25$  a total of three times (with the first such loading indicated by the black dashed curve in Fig. 2), followed by compression to a higher strain of  $\varepsilon = 0.6$ . The present model is able to capture the occurrence and the magnitude of the shift to the right of the stress–strain response that follows material preconditioning at  $\varepsilon = 0.25$ , as a result of microstructural rearrangements (“damage”). We were able to roughly approximate the experimental behavior by assuming  $k_0 = 3.91 \times 10^6$  Pa,  $k_c = 12.4k_0$ ,  $\varepsilon_* = 0.55$ , loading plateau at  $\sigma = 2.2 \times 10^6$  Pa, and unloading plateau at  $\sigma = 0.2 \times 10^6$  Pa. Additionally, we set  $\beta = 1$  for the loading cycle from the virgin state, and  $\beta = 0.925$  for the loading cycle after the preconditioning at  $\varepsilon = 0.25$  (refer to the solid curves shown in Fig. 2 for the limiting stress–strain response corresponding to such material parameters). The most notable difference between the numerical predictions of the present model and the experimental data is the perfectly horizontal loading/unloading plateaux of the former and the significant sloping of these regions in the latter. This discrepancy arises because the model discussed herein assumes a uniformity of material properties (c.f. Assumptions (A1) and (A2)) along the height of the CNT array as a simplification, when in fact it is known that CNT arrays can have gradients in physical properties along their



**Fig. 1.** Numerical overall stress–strain response of bistable mass-spring chains for different total number of springs  $N$ .



**Fig. 2.** Simulation of experimental data in which a CNT array was compressed to a moderate strain of  $\varepsilon = 0.25$  (first cycle in black), followed by compression to a larger strain of  $\varepsilon = 0.6$  (in red). (For interpretation of the references to color in this figure legend, the reader is referred to the web version of the article.)

height as a side effect of the synthesis process (Cao et al., 2005; Raney et al., 2011b). The use of “hardening” type plasticity would allow us to more accurately predict the switching point from phase  $a$  to phase  $b$ , and the actual dissipative behavior of CNT arrays. In Fraternali et al. (2010) and Raney et al. (2011a) we have employed loading and unloading hardening parameters to successfully model this aspect of the experimental data, but here we do not repeat the use of that approach for the sake of brevity.

#### 4. Concluding remarks

In this paper, for the first time a bistable-spring ansatz has been proposed capable of incorporating damage in plastically deformed materials.

We have shown that a suitable modification of the model recently proposed by Fraternali et al. (2010) for CNT foams is able to handle preconditioning-induced material damage, which is characterized by an activation strain different from zero; a reduction in the energy dissipation capacity; and permanent deformation. The latter, in particular, coincides with the activation strain. The new model allows us to extend the ‘transformational plasticity’ concept discussed by Puglisi and Truskinovsky (2005) from time-independent hysteretic behavior to fatigue-type material damage. It applies to a wide class of materials showing Mullins-like behavior (Mullins, 1947), which includes besides CNT arrays rubber-like and soft biological materials.

We address a multiscale formulation of the present model, accounting for graded mechanical properties along the height of the structure (Raney et al., 2011a), and the analytic computation of the energy dissipated by the system in the continuum limit in future work.

#### Acknowledgements

FF acknowledges the support of the Province of Avellino through the grant “Innovative systems for seismic engineering and structural health monitoring”. TB acknowledges the support of the German Research Community (DFG) through grant BL 512 4/1. JRR gratefully acknowledges the U.S. Department of Defense and the Army Research Office for their support via a National Defense Science & Engineering Graduate (NDSEG) fellowship. CD acknowledges support from the Institute for Collaborative Biotechnologies under contract W911NF-09-D-0001 with the Army Research Office.

#### References

Baughman, R.H., Zakidov, A.A., de Heer, W.A., 2002. Carbon nanotubes—the route toward application. *Science* 297 (5582), 787–792.

- Blesgen, T., 2007. The competition of elastic energy and surface energy in discrete numerical systems. *Advances in Computational Mathematics* 27, 179–194.
- Bradford, P.D., Wang, X., Zhao, H., 2011. Tuning the compressive mechanical properties of carbon nanotube foam. *Carbon* 49, 2834–2841.
- Braides, A., 2002. *Gamma-convergence for Beginners*, Oxford Lecture Series in Mathematics. Oxford University Press.
- Braides, A., Dal Maso, G., Garroni, A., 1999. Variational formulation of softening phenomena in fracture mechanics: the one-dimensional case. *Archive for Rational Mechanics and Analysis* 146, 23–58.
- Cao, A., Dickrell, P., Sawyer, W.G., Ghasemi-Neihad, M., Ajayan, P., 2005. Supercompressible foam-like carbon nanotube films. *Science* 310, 1307–1310.
- De Tommasi, D., Puglisi, G., 2006. A micromechanics-based model for the Mullins effect. *Journal of Rheology* 50 (4), 495–512.
- Dorfmann, A., Ogden, R.W., 2004. A constitutive model for the Mullins effect with permanent set in particle-reinforced rubber. *International Journal of Solids and Structures* 41, 1855–1878.
- Fraternali, F., Blesgen, T., Amendola, A., Daraio, C., 2010. Multiscale mass-spring models of carbon nanotube foams. *Journal of the Mechanics and Physics of Solids* 59 (1), 89–102.
- Gibson, L.J., Ashby, M.F., 1999. *Cellular Solids: Structure and Property*, 2nd ed. Pergamon Press, Oxford.
- Hutchens, S.B., Hall, L., Greer, J.R., 2010. In situ mechanical testing reveals periodic buckle nucleation and propagation in carbon nanotube bundles. *Advanced Functional Materials* 20, 2338–2346.
- Misra, A., Greer, J., Daraio, C., 2009. Strain rate effects in the mechanical response of polymer anchored carbon nanotube foams. *Advanced Materials* 21, 334–338.
- Mullins, L., 1947. Effect of stretching on the properties of rubber. *Journal of the Rubber Research* 16 (12), 275–289.
- Puglisi, G., Truskinovsky, L., 2002. Rate-dependent hysteresis in a bi-stable chain. *Journal of the Mechanics and Physics of Solids* 50 (2), 165–187.
- Puglisi, G., Truskinovsky, L., 2005. Thermodynamics of rate-independent plasticity. *Journal of the Mechanics and Physics of Solids* 53 (3), 655–679.
- Raney, J.R., Fraternali, F., Amendola, A., Daraio, C., 2011a. Modeling and in situ identification of material parameters for layered structures based on carbon nanotube arrays. *Composite Structures* 93 (11), 3013–3018.
- Raney, J.R., Misra, A., Daraio, C., 2011b. Tailoring the microstructure and mechanical properties of arrays of aligned multiwall carbon nanotubes by utilizing different hydrogen concentrations during synthesis. *Carbon* 49 (11), 3631–3638.
- Rockafellar, R., 1997. *Convex Analysis*, 2nd ed. Princeton University Press.
- Yaglioglu, O., 2007. *Carbon Nanotube Based Electromechanical Probes*. PhD thesis. Massachusetts Institute of Technology, Cambridge, MA.